Optimal Deployment for Magnetic Induction-Based Wireless Networks in Challenged Environments

Zhi Sun, *Member, IEEE,* and Ian F. Akyildiz, *Fellow, IEEE*

***Abstract*—New propagation techniques using magnetic induction (MI) waveguide solves the problems of traditional techniques in many challenged environments, such as underground, mines/tunnels, and oil reservoirs. However, deploying MI waveguides to connect the wireless nodes in such networks is challenging due to the high deployment cost, the complex shape of the communication range of the MI waveguides, and the significant impacts of the node failure and relay coil displacement. To date, the deployment problems in the MI-based networks have not been addressed. In this paper, the optimal MI waveguide deployment strategies are investigated in both one and two dimensional MI-based networks where the nodes are distributed either randomly or according to a regular lattice. Validated by both theoretical deduction and simulations, the proposed deployment strategies can construct a reliable MI-based network that is robust to node failure and relay coil displacement with minimum cost.**

***Index Terms*—Magnetic induction communications, optimal deployment, challenged environments, network topology.**

I. Introduction

In challenged environments, such as underground, mines/tunnels, and oil reservoirs, the wireless networks enable a large variety of novel and essential applications, including: intelligent irrigation, earthquake and landslide forecast, mine disaster prevention and rescue, underground pipeline monitoring, oil recovery, concealed border patrol, among others [1], [6], [7]. Despite the potential advantages, due to the hostile transmission medium of the challenged environments, the well-established existing wireless networks do not work well [1].

Most existing wireless networks use the electromagnetic (EM) waves for signal propagation. However, the EM waves encounter two major problems in the challenged environments, including the extremely small communication range and the highly dynamic channel conditions [1]. To address the above problems, in [2], [3], we developed the *Magnetic Induction (MI) waveguide* technique. As shown in Fig. 1, the wireless communications are accomplished by the consecutive magnetic induction between adjacent MI relay coils. The sinusoidal current in the transmitter coil first creates a time varying magnetic field, which can induce another sinusoidal current in the first relay coil, so on and so forth. By this way, the magnetic induction can be passively relayed by the multiple coils until reaching the MI receiver, forming the so called MI waveguide. The MI waveguide technique solved the problems in EM wave-based techniques and provide more favorable advantages for the wireless networks in challenged environments: 1) The communication range is greatly enlarged. For example, in soil medium, the range increases from less than 4 m to more than 100 m [2]. 2) The MI channel conditions remain constant in most transmission media, since the attenuation rate of the magnetic fields does not change in non-magnetic media. 3) The MI relay coils do not consume extra energy and the unit cost is neglectable. Those coils are easy to deploy and do not need regular maintenances. 4) The system lifetime can be greatly prolonged since the MI-based devices can be recharged wirelessly using the inductive charging technique.

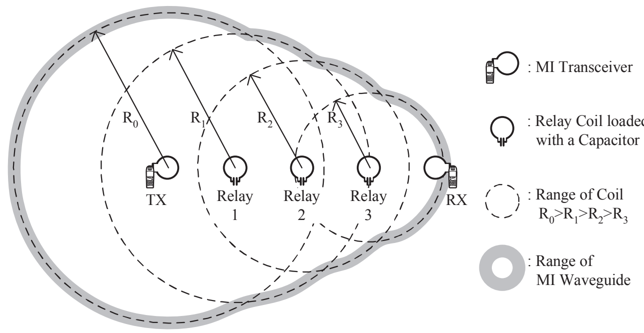

Fig. 1. The structure and the communication range of a MI waveguide.

Although the MI waveguide technique solves the point-to-point communication problem in the challenged environments, how to deploy the MI waveguides to connect a large number of wireless nodes is challenging. Specifically, due to the hostile transmission medium, all nodes in the network are isolated unless they are connected by MI waveguides. Hence, the MI waveguide deployment strategy design is essential to realize the MI-based wireless communications among multiple MI nodes. On the one hand, a non-trivial number of relay coils are required to construct a connected and robust wireless network. On the other hand, the intensive deployment of the coils in the challenged environments costs a great amount of labor. Therefore, the objective of the deployment strategy in MI-based wireless networks is to *construct a connected and robust network with as few relay coils as possible*. To achieve this goal, three fundamental deployment questions need to be addressed:

Manuscript received October 22, 2011; revised August 21, 2012; accepted November 21, 2012. The associate editor coordinating the review of this paper and approving it for publication was S. Valaee.

Z. Sun is with the Department of Electrical Engineering, State University of New York at Buffalo, Buffalo, NY 14260, United States (e-mail: zhisun@buffalo.edu).

I. F. Akyildiz is with the School of Electrical and Computer Engineering, Georgia Institute of Technology, Atlanta, GA 30332, United States (e-mail: ian@ece.gatech.edu).

A much shorter preliminary version of this paper appeared in [4].

Digital Object Identifier 10.1109/TWC.2013.011713.111896

- *What is the topology and position of each MI waveguide?* Unlike the disk-shaped communication range of the traditional wireless devices, the range shape of the MI waveguide is more complicated due to the consecutive passive magnetic inductions, as shown in Fig. 1. Hence, the deployment strategies in the MI-based networks are completely different. The topology and the position of each MI waveguide need to be carefully designed.
- *How many relay coils are needed?* The waveguide topology/position and the number of relay coils constituting each MI waveguide should be jointly designed to minimize the total relay coil number while guaranteeing the expected network robustness.
- *How robust is the constructed MI-based wireless network?* Since the communication success of the MI waveguide relies on multiple resonant relay coils, the functionality of the MI-based network depends on not only the wireless nodes but also all the relay coils. The system robustness to the node malfunction and the coil position deviation needs to be characterized.

To the best of our knowledge, these questions have not been addressed so far. Moreover, instead of being limited to heuristics, it is more important to develop the deployment solutions that can be rigorously proved to be optimal in terms of robustness and low-cost.

In this paper, we theoretically investigate the optimal MI waveguide deployment strategies for the MI-based wireless networks in challenged environments. In particular, we start with the MI waveguide deployment in one-dimensional (1D) networks. The optimal number of relay coils for a 1D MI link is derived to capture the effects of multiple system parameters, including the transmission distance, operating frequency, coil size, and coil deviations. Then we focus on the deployment strategy for the two-dimensional (2D) MI networks. Since the 2D network is constituted by 1D links, the 2D deployment strategy is based on the strategy in 1D networks. We consider the 2D networks where the wireless nodes are either randomly distributed or located on a regular lattice. We propose a MI waveguide deployment algorithm by utilizing the Voronoi diagram and the Fermat point [5], which is proved to be optimal to trade off between the total number of relay coils and the network robustness to device failure and coil displacement. The effectiveness of the proposed deployment strategy is validated by both theoretical deduction and computer simulations.

The remainder of this paper is organized as follows. In Section II, the related works are introduced. In Section III, the optimal MI waveguide deployment strategy is developed in both 1D and 2D networks. Then, in Section IV, numerical studies are performed. Finally, the paper is concluded in Section V.

II. Related Work

The MI-based communication technique were first introduced as an alternative to the Bluetooth in [9]. The rapid attenuation of the magnetic field strength is exploited to eliminate the mutual interference. However, the high path loss is obviously not an advantage in the proposed applications in the challenged environments. The MI waveguide technique is first developed in [10], [11], which is designed as artificial delay filters, dielectric mirrors, distributed Bragg reflectors, slow-wave structures, coupled cavities, among others. In [2], [3], we first utilize the MI waveguide in the field of wireless communications, which can greatly enlarge the communication range in many challenged environments. It should be noted that we adopt a theoretical propagation model that is similar as in [11]. This model has been validated by experiments in [12].

The deployment problem in the MI-based wireless networks is related to the topology control problem in the traditional wireless networks. In [13], a robust and energy-efficient wireless network is constructed by adjusting the transmission power of each wireless node. In [14], a topology control strategy is proposed to guarantee connectivity in a wireless network while the interference is minimized. In [15], an energy-aware topology control algorithm for a hierarchical sensor network is proposed. In [16], a comprehensive survey on the topology control protocols that utilize the geometric structures and virtual backbones is provided. In [17], the virtual force algorithm is introduced for wireless sensor networks. In [18], the Voronoi diagram-based mobile sensor deployment protocols are proposed to discover and fill the coverage holes. All the above works focus on the wireless networks that use traditional EM wave-based techniques. None of the existing works can address the deployment problems in the MI-based networks, which have fundamental differences: 1) the nodes in traditional wireless networks can directly connect to each other while the nodes in the MI-based network can only be connected through the MI waveguides; and 2) the nodes in traditional wireless networks have disk-shaped communication range while the MI waveguide in the MI-based network has a much more complicated communication range, as shown in Fig. 1. In this paper, we investigate the optimal MI waveguide deployment strategy to construct a low-cost and fully connected MI-based network that is robust to device failures and coil displacements in challenged environments.

III. Optimal MI Waveguide Deployment Algorithm

In this section, the optimal MI waveguide deployment strategy is developed for the MI-based wireless networks in challenged environments. Specifically, we start with the deployment strategy in the basic 1D networks and then focus on the optimal deployment in the more general 2D networks. Since the 2D networks is constituted by multiple 1D links, the analysis results of the 1D deployment strategy lay the foundation of the MI waveguide deployment strategy in 2D MI-based networks. It should be noted that this paper focuses on the deployment strategy to construct a fully connected MI network. The interferences between multiple MI transceivers are assumed to be effectively eliminated by some well designed MAC/scheduling protocols, which we have analyzed in another paper [8].

A. MI Waveguide Deployment in 1D MI-based Networks

In 1D networks, the wireless nodes are located along a polygonal line. This type of network topology is suitable for many applications where the wireless nodes are placed along a chain, such as the underground pipeline monitoring system

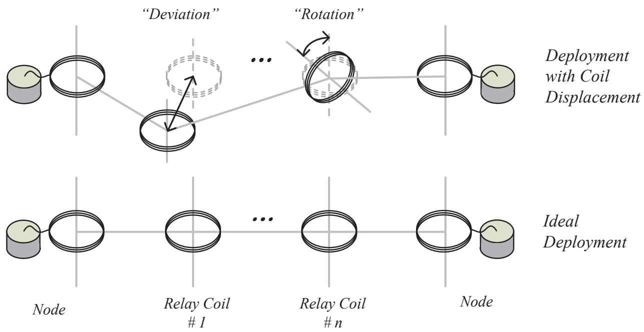

Fig. 2. Illustration of the possible relay coil displacements.

and the border patrol system. The 1D networks can be divided into multiple links connecting adjacent nodes. The goal of MI waveguide deployment in 1D network is to use as few relay coils as possible to connect the two nodes in each link. A certain level of robustness to the node failure and coil displacement is also required. The optimal number of relay coils for each link is determined by path loss of the link, which is the function of the length of the link, the coil parameters, and the expected network reliability. In this subsection, we first give the path loss of the MI waveguide communications and then use the derived path loss to calculate the optimal relay coil number of each 1D link.

1) Path Loss of the MI Waveguide under the Impact of Coil Displacement: In [2], [3], the path loss of the ideally deployed MI waveguide are provided. In this subsection, we extend the results to cover the scenarios when the relay coils constituting the MI waveguides are randomly displaced from the ideal positions. Assuming that the length of a link is d. An MI waveguide with $n-1$ relay coils is deployed along the link. The angle frequency of the signal is ω. In the ideal case, the relay coils are placed horizontally in a planar line, as shown in Fig. 2. This MI waveguide structure guarantees the omnidirectional coverage of each relay coil, which eases the deployment of the coils in the challenged environments. The ideal intervals r_i $(i = 1, 2, ...n)$ between every two adjacent relay coils are all the same and $r_i = d/n$.

However, in the practical operations, the position of each coil in the MI waveguide may deviate from the ideal positions due to the perturbations in the challenged environments. As shown in Fig. 2, the horizontal and vertical deviation as well as the rotation of each coil may cause the changes of the coil intervals r_i and the axial directions of each coil. As a result, the mutual inductions M_i $(i = 1, 2, ...n)$ between adjacent relay coils may be different:

$$M_i \simeq \mu \pi N^2 \frac{a^4}{4r_i^3} \cdot (2 \sin\theta_{t_i} \sin\theta_{r_i} + \cos\theta_{t_i} \cos\theta_{r_i}) \tag{1}$$

where μ is the medium permeability; N is the number of turns of the coils; a is the coil radius; θ_t and θ_r are the angles between the coil radial directions and the line connecting the coil centers.

Then based on the results provided in [2], [3], the path loss (in dB) of the MI waveguide under the impact of coil displacement can be expressed as

$$L_{MI}(d, n, \omega) \simeq 6.02 + 20\lg\left[\frac{Z}{\omega M_n} \cdot \zeta(\tfrac{Z}{\omega M_i}, n-1)\right], \tag{2}$$

where Z is the self impedance of one relay coil; ω is the operating angular frequency; and $\zeta(\frac{Z}{\omega M_i}, n)$ is a polynomial of $\frac{Z}{\omega M_i}$ $(i = 1, 2, ...n)$. The self impedance of a coil Z is designed to be resonant at the center frequency ω_0. When $\omega = \omega_0$, Z becomes pure resistance R, which is the coil wire resistance. The polynomial $\zeta(\frac{R}{\omega M_i}, n)$ can be developed as

$$\begin{aligned}
&\zeta(\tfrac{R}{\omega M_i}, 0) = 1 \,, \\
&\zeta(\tfrac{R}{\omega M_i}, 1) = \frac{R}{\omega M_1} + \frac{\omega M_1}{R} \,, \\
&\quad\vdots \\
&\zeta(\tfrac{R}{\omega M_i}, n) = \frac{R}{\omega M_n} \cdot \zeta(\tfrac{R}{\omega M_i}, n-1) + \frac{M_n}{M_{n-1}} \cdot \zeta(\tfrac{R}{\omega M_i}, n-2) \,.
\end{aligned} \tag{3}$$

Substituting (3) into (2) yields the path loss of the MI waveguide under the impact of coil displacement. It should be noted that the mutual induction M_i are random variables due to the random coil displacement. Consequently, the path loss is also a random variable.

2) Optimal Number of Relay Coils: To minimize the deployment cost and guarantee the network working properly most of the time, the MI waveguide should use the minimum number of relay coils to maintain a very low probability that its path loss is smaller than a threshold. To derive such optimal number, the complicated link path loss given in (3) and (2) need to be simplified first. In (3), the value of $\frac{R}{\omega M_i}$ is large enough, especially in the case that the coil interval r_i is set as large as possible in order to reduce the coil number. Since $\zeta(\frac{R}{\omega M_i}, n)$ is a polynomial of $\frac{R}{\omega M_i}$, the highest order variable in the polynomial has the most influence. Therefore, (3) can be approximately expressed as:

$$L_{MI}(d, n, \omega) \simeq 6.02 + 20\lg\left(\prod_{i=1}^{n} \frac{R}{\omega M_i}\right), \tag{4}$$

Assuming that the transmission power of each node is p_t and the minimum received power for correctly demodulation is p_{th} (both in dBm). We expect that the MI waveguide link has the outage probability (i.e. the received power is smaller than the threshold) smaller than P_{outage}:

$$P\left(p_t - L_{MI}(d, n, \omega) < p_{th}\right) < P_{outage}. \tag{5}$$

If the optimal relay coil number is denoted as n_{opt}, according to the previous discussion and substituting (4) into (5), we have:

$$P\left(p_t - 6.02 - 20\lg\left(\prod_{i=1}^{n_{opt}} \frac{Z}{\omega M_i}\right) < p_{th}\right) = P_{outage}. \tag{6}$$

Therefore,

$$P\left(\prod_{i=1}^{n_{opt}} M_i < \frac{(\frac{R}{\omega})^{n_{opt}}}{10^{\frac{p_t - 6.02 - p_{th}}{20}}}\right) = P_{outage}. \tag{7}$$

If all relay coils are fixed at the ideal positions, the coil interval is fixed at $r_i = d/n_{opt}$. Hence, all the mutual inductions M_i are the same and the path loss is a determined value.

Therefore, in case of the ideal deployment, the optimal number of relay coils for a link should fulfill the following equation:

$$n_{opt}(d, B) = \arg\min_{n}\{P_t - L_{MI}(d, n, \omega_0 + 0.5B) \geq P_{th}\}. \tag{8}$$

Due to the random coil deviation, the mutual inductions M_i of all links are random variables. The distribution of M_i is influenced by many perturbations determined by the geographic characteristics and specific applications. Hence, the exact distribution functions of M_i is very complicated and different from case to case. In this paper, we approximately model the distribution of M_i to shed a light on how the coil displacement influences the network reliability and the optimal coil number. We model the M_i of each link as independent and identical random variables that are uniformly distributed in the interval $[M_{min}, M_{max}]$. The value of M_{min} and M_{max} are determined by the intensity of the coil displacement. According to (1), the coil displacement may change the coil interval r_i and directions θ_t, θ_r. The term $(2\sin\theta_{t_i}\sin\theta_{r_i} + \cos\theta_{t_i}\cos\theta_{r_i})$ ranges from 0 to 2 and is 1 when coils are ideally placed. The term r_i ranges from d/n to infinity and is d/n when coils are ideally placed. Therefore, if the coil displacement intensity is $a\%$, M_i is uniformly distributed in the interval $[M_{min}(d, n, b\%), M_{max}(d, n, b\%)]$, where

$$M_{min}(d, n, b\%) = \mu\pi N^2 \frac{a^4}{4[\frac{d}{n}(1 + b\%)]^3} \cdot (1 - b\%)$$
$$M_{max}(d, n, b\%) = \mu\pi N^2 \frac{a^4}{4(\frac{d}{n})^3} \cdot (1 + b\%). \tag{9}$$

Since M_i are uniform, independently and identically distributed random variables, the probability density function (PDF) of $X = \prod_{i=1}^{n} M_i$ can be expressed as [19]:

$$f_X(x)=\begin{cases} \sum_{j=0}^{n-k} \frac{(-1)^j}{(M_{max}-M_{min})^n (n-1)!}\binom{n}{j}\left(\ln \frac{{M_{max}}^{n-j}{M_{min}}^{j}}{x}\right)^{n-1}, & \\ \quad \text{if } {M_{min}}^{n-k+1}{M_{max}}^{k-1} \leq x \leq {M_{min}}^{n-k}{M_{max}}^{k}, \; k=1, ..., n & \\ 0, \quad \text{else} & \end{cases} \tag{10}$$

Then (7) can be developed as

$$P\left(\prod_{i=1}^{n_{opt}} M_i < \frac{(\frac{R}{\omega})^{n_{opt}}}{10^{\frac{p_t-6.02-p_{th}}{20}}}\right) = \int_{{M_{min}}^n}^{\frac{(\frac{R}{\omega})^{n_{opt}}}{10^{\frac{p_t-6.02-p_{th}}{20}}}} f_X(x)\,dx = P_{outage}. \tag{11}$$

By substituting (10) and (9) into (11), the optimal relay coil number can be derived by numerically solving the resulted transcendental equation. The optimal number of relay coils is the function of the link length d, the outage probability P_{outage}, the displacement intensity $b\%$, the operating frequency ω, and the coil parameters such as the coil size, number of turns, and wire resistance. Since usually the outage probability, the operating frequency, and the coil parameters are fixed, the only variables in deployment design are the link length and the displacement intensity.

By using the parameters of the MI waveguide developed in [2], we can numerically analyze the optimal number of relay coils with different link length and displacement intensity. In the numerical analysis, the transmission power is 2.5 mW (4 dBm). The power threshold for correctly reception is -90 dBm. The maximum tolerable outage probability is 5%.

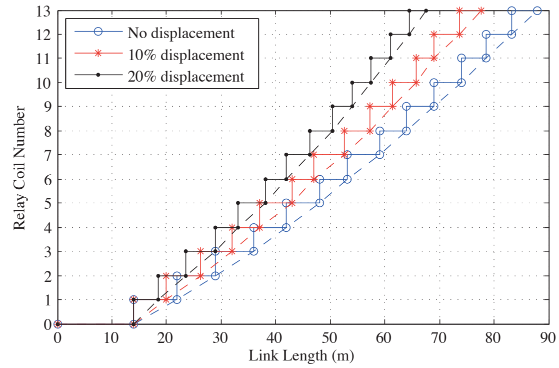

Fig. 3. Optimal relay coil number with different link length and displacement intensity.

The operating frequency is 10 MHz. The relay coils have the same radius of 0.15 m and the number of turns is 20. The wire resistance of unit length is 0.01 Ω/m. The MI-based wireless network is deployed in soil medium. The permeability is a constant and is similar to that of the air, since most soil in the nature does not contain magnetite. Therefore, $\mu = 4\pi\times10^{-7}$ H/m. The soil moisture and the soil composition do not affect the MI communication as discussed perviously.

In Fig. 3, the optimal number of relay coils for one link in a 1D MI-based network with different coil displacement intensities are shown as a step function of the link length. Since the dashed line connecting each step constitutes a convex function, the optimal relay coil number increases faster than the link length. This phenomenon is due to the fact that the coils relay the signal in a passive way and no extra power is added at each relay coils. If coil displacements exist, a dramatically larger coil number is required to keep the outage probability low. As the displacement intensity increases, the required coil number increases even faster. Moreover, the coil displacement has more obvious impacts when link length increases. Hence, both the link length and the coil displacement should be kept below a threshold.

Besides the coil displacements, it should be noted that the 1D network is very sensitive to the node failure, since the network will be partitioned into disconnected parts if any node dies. To enhance the robustness to node failure in 1D network, the only solution is to use MI waveguide to connect multi-hop neighbors. The same equations can be used to calculate the optimal coil number. The only difference is that the parameter d is changed to the sum of multiple links.

B. Topology Model of the 2D MI-based Networks

In most applications, the network is deployed in a 2D plane, such as the intelligent irrigation system, the earthquake and landslide forecast system, and the mine disaster prevention and rescue system, among others. In the remainder of this section, we investigate the deployment strategies of the MI waveguides to connect the nodes in a 2D network. Compared with 1D networks, the deployment in 2D networks is much more complicated: 1) in 1D networks, the route connecting the wireless nodes are determined, i.e. the path connecting the nodes along the 1D polygonal line. In contrast, the optimal route to connect all the wireless nodes in the 2D plane needs to be found out; and 2) it is possible in a 2D network that some common relay coils can be shared by multiple links so that the total number of relay coils can be reduced.

The positions where the MI waveguides are deployed are first determined by the distribution of the nodes, which can be divided into two categories: the random and the regular distribution. If the nodes can be placed at any desired positions, the regular distribution, such as the hexagonal tessellation, can be used due to the high efficiency and simplicity. Otherwise, if the nodes has to be placed at certain positions due to environmental constraints or application requirements, the node distribution is random. In the rest part of this section, we first investigate the optimal deployment in the general case, i.e. the 2D MI-based network with random node distribution. Then we focus on the special case, i.e. the network with regular node distribution, to achieve more explicit results.

C. MI Waveguide Deployment in 2D Networks with Random Node Distribution

As discussed previously, the objective of the optimal deployment includes: 1) using as few as relay coils as possible and 2) constructing a network as robust as possible to the node failure and the coil displacement. In this subsection, we investigate the optimal deployment strategies for the 2D MI-based networks with random node distribution. The positions of the wireless nodes in such 2D networks are supposed to follow a homogenous Poisson point process with the spatial density λ_{rand} (m^{-2}). We first propose a minimum spanning tree (MST) algorithm, which can minimize the total relay coil number but is not robust at all. The constructed network is not efficient in power consumption and routing, either. To address the problem, we propose a Voronoi diagram-based route, which achieves optimal balance between system robustness and cost. The constructed network topology is also geometrical and power spanner. Finally, we provide a Fermat point-based method to further reduce the deployment cost without losing the spanner property and the robustness.

1) Minimum Spanning Tree (MST) Deployment Algorithm: If the robustness is not considered, the most important goal is to connect all the nodes with minimum number of relay coils. To this end, the minimum spanning tree [20] can be used to establish a connected MI-based wireless network, where the weight of each edge is the optimal relay coil number given in Section III-A2.

According to the properties of the minimum spanning tree, the MST algorithm can construct a connected MI-based network with minimum number of relay coils. However, the failure of any one node disconnects the whole network. Moreover, the network is disconnected if the outage caused by the coil displacement happens in any one MI waveguide. In addition, the spanning tree topology may cause high congestions and end-to-end power consumption. Therefore, although the MST algorithm achieves the minimum deployment cost, it is not the optimal strategy.

2) Voronoi Diagram (VD)-based Deployment Route: To find the optimal deployment strategy, we first identify the metrics to quantitatively characterize the robustness. The most accurate metric is the network outage probability, i.e. the probability that the data transmission from an arbitrary source to an arbitrary destination is failed due to the disconnected network. However, since the node distribution is highly random, it is impossible to derive the analytical expression of the network outage probability. Hence, we use a more straightforward network parameters, the average node degree (1-hop neighbor number), to characterize the network robustness. Since the node distribution follows a homogenous Poisson point process, the average node degree can to a large extend represent the network outage behavior. Then, the deployment objective becomes to find the optimal balance between the small coil number and the large node degree. The constructed network should also be efficient in reducing congestions and the power consumption.

To this end, we propose the Voronoi diagram-based route, along which the MI waveguides are deployed. As shown in Fig. 4, the Voronoi diagram of the wireless nodes partitions the whole area into Voronoi cells. Each cell contains one node. Any point in one Voronoi cell is closer to the node in this cell than to any other nodes. The Voronoi diagram-based route is constructed by connecting the nodes in adjacent cells, as shown in Fig. 4. Then the MI waveguides are deployed along this Voronoi diagram-based route. If every transmission pair has to use a unique MI waveguide, the Voronoi diagram-based route is optimal due to the following properties:

Proposition 1. *The average node degree of the MI-based network constructed by the Voronoi diagram-based route is approximately* 6*.*

The proof of proposition 1 is given in Appendix A. According this proposition, the Voronoi diagram-based route achieves a much higher average node degree ($E(m) = 6$) than the MST algorithm ($E(m) \simeq 2$). Since the network robustness increases exponentially with the node degree, the Voronoi diagram-based route significantly enhances the robustness, which is also clearly shown in the numerical studies in Section IV.

Next, we quantitatively exam the balance between the deployment cost and network robustness. We define a new matric, the *cost-robust factor* $\rho_{cost-robust}$, to characterize such balance, which is the ratio of average coil number per node to average node degree in the constructed network. The smaller $\rho_{cost-robust}$ is, the higher cost-robust efficiency. Then we have the following proposition.

Proposition 2. *The average cost-robust factor of the network with the Voronoi diagram-based route is in the same order of that in the network constructed by the MST algorithm.*

The proof of proposition 2 is given in Appendix B. Proposition 1 and 2 indicate that the Voronoi diagram-based route achieves much higher network robustness than the MST algorithm by introducing reasonable number of relay coils.

Besides the network robustness, the congestions and power consumption should be also considered. Hence, we introduce the following propositions:

Proposition 3. *The MI-based network constructed according to the Voronoi diagram-based route is planar and geometrical spanner.*

As mentioned before, the Voronoi diagram-based route forms a Delaunay triangulation, which has been proved to be planar and geometrical spanner [16]. Therefore, Proposition 3 is proved.

The geometrical spanner property indicates that the shortest path connecting any two nodes in the constructed MI-based network is not longer than k ($k < \infty$) times of the Euclidean distance between them. This property guarantees that the data between any source and destination nodes can be transmitted through a relatively short path, which is necessary for the power efficiency, quality of service, and reliability of the MI-based wireless networks. Moreover, the planar property of the resulted network is preferred for most geographic routing protocols, which is favorable for those resource-limited devices [16]. In the traditional wireless networks, it has been proved that the network with a Delaunay triangulation topology is also power spanner, i.e., the total power consumption along the shortest path connecting any two nodes in such network is not much larger than the power consumption of the direct transmission between them. In wireless networks using MI waveguides, due to the complete different channel model, the power spanner property needs to be reexamined. Therefore, we have the following proposition:

Proposition 4. *The MI-based network with Voronoi diagram-based route is also power spanner.*

The proof of proposition 4 is given in Appendix C. According to Proposition 3 and 4, the MI-based networks with the Voronoi diagram-based route achieve similar routing, congestion, and power consumption performance as the network with the complete graph topology. To guarantee the spanner properties, no edge on the route should be deleted. Similarly, to guarantee the planar properties, no edge can be added, either.

3) Further Improvement based on the Fermat Point: The Voronoi diagram-based route significantly enhance the network robustness by adding reasonable number of relay coils. It also improve the routing and energy performance due to the planar and spanner properties. If we assume that each link has to use a unique MI waveguide, the Voronoi diagram-based route is optimal for the MI waveguide deployment. If this constraint can be released, i.e., multiple links can share the same sets of relay coils, the relay coil number can be further reduced.

Our objective is to reduce the coil number but keep the same network topology of the Voronoi diagram-based route. To this end, we propose the Fermat point-based improvement: the three MI waveguides along the edges in each Delaunay triangle cell can be replaced by one MI waveguide with a shape of the three-pointed star, as shown in Fig. 4. The nodes on all the three vertexes can use the same waveguide to communicate with each other directly. The center of the three-pointed star is located at the Fermat point of the triangle. Since the total distance from the three vertices to the Fermat point is the minimum possible [5], the three-pointed star MI waveguide centered at the Fermat point consumes the minimum number of coils to connect the three nodes.

To construct a network with the same topology as the original Voronoi diagram-based route, the three-pointed star shaped MI waveguides only need to be deployed in every other Delaunay triangle cells, as shown in Fig. 4. By this way, the relay coil number required to construct the Voronoi diagram-based route is significantly reduced. Meanwhile, the network topology and the robustness to node failure remain the same since all the original links are not affected. It should be noted that the robustness to coil displacement is slightly weakened since every three links share the same MI waveguide. However, the impacts of coil displacement can be limited to a very small extent according to the optimal deployment strategy in Section III-A. Hence the total network robustness can be viewed to be the same as the original Voronoi diagram-based route.

To sum up, the deployment strategy using both Voronoi diagram-based route and the Fermat point-based improvement achieves high network robustness as well as low congestions and power consumption with minimum relay coil number. We denote this optimal deployment as Voronoi-Fermat (VF) algorithm. The detailed procedure of the VF algorithm is described in Fig. 5.

Create the Voronoi diagram of the K wireless nodes, and derive K Voronoi cells $\mathbf{VC} = \{VC_1, VC_2, ..., VC_K\}$.
Keep a subset $\mathbf{G}$ of $\mathbf{VC}$; $\mathbf{G}$ initially contains VC_1.
while (Not all Voronoi cells are in $\mathbf{G}$) **do**
  Find a Voronoi cell VC_x in $\mathbf{G}$ that has the neighbor Voronoi cells $\{VC_x^1, VC_x^2, ..., VC_x^j\}$ which are not in $\mathbf{G}$.
  Connect the adjacent wireless nodes in $\{VC_x^1, VC_x^2, ..., VC_x^j\}$ and VC_x, and derive the non-overlapped triangle cells $\{Tr_1, Tr_2, ..., Tr_{j-1}\}$.
  if (j is odd) **then**
    In triangle cells $Tr_1, Tr_2, Tr_4, ..., Tr_{j-1}$, deploy the MI waveguide along the three lines connecting the vertexes and the Fermat point.
  else
    In triangle cells $Tr_1, Tr_3, Tr_5, ..., Tr_{j-1}$, deploy the MI waveguide along the three lines connecting the vertexes and the Fermat point.
  end if Add $\{VC_x^1, VC_x^2, ..., VC_x^j\}$ to $\mathbf{G}$.
end while

Fig. 5. Voronoi-Fermat (VF) algorithm for MI waveguide deployment

D. MI Waveguide Deployment in 2D Networks with Hexagonal Tessellation Topology

Based on the deployment analysis in the general scenario with random node distribution, in this subsection, we focus on the special scenario where the nodes are distributed with regular patterns, especially the hexagonal tessellation. More explicit expressions can be derived due to the regular pattern. Hexagonal tessellations have been widely used for the traditional wireless network topologies, such as the base station placement of the cellular networks due to the efficiency in coverage. In the following analysis, we assume that the node density of the MI-based network with the hexagonal tessellation topology is λ_{hex} (m^{-2}).

1) Minimum Spanning Tree (MST) Algorithm: Similar in the network with random node distribution, the MST algorithm can be used to minimize the relay coil number without considering the network robustness. The average neighbor number of the resulted network is approximately 2, which is the same as in the random node distribution scenario.

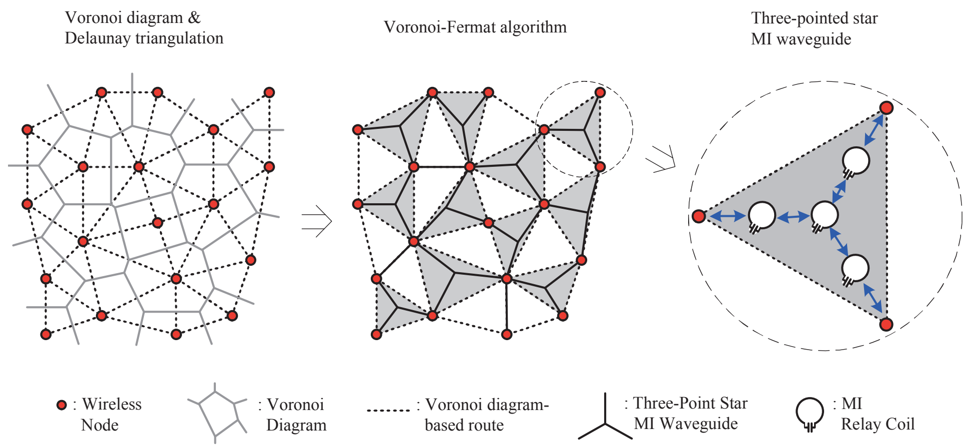

Fig. 4. The MI waveguide deployment using VF algorithm in the MI-based networks with random node distribution.

Next we calculate the cost-robust factor $\rho_{cost-robust}$. If the total number of wireless node is K, the total number of links in the minimum spanning tree is $K-1$. The edges of the hexagonal tessellation have the same length d^{hex}, which is determined by the node density λ_{hex}:

$$d^{hex} = 2 \cdot 3^{-\frac{1}{4}} \cdot \lambda_{hex}^{-\frac{1}{2}}\,, \tag{12}$$

By utilizing the strategy given in Section III-A, the optimal number of relay coils n_{opt} for each link can be calculated as a function of link length d^{hex} and the tolerable outage probability p_{coil}^{out} for a single MI waveguide. Then the total number of the relay coils to connect the K wireless nodes based on the MST algorithm is

$$Num_{mst}^{hex} = (K-1) \cdot n_{opt}(2 \cdot 3^{-\frac{1}{4}} \cdot \lambda_{hex}^{-\frac{1}{2}}, p_{coil}^{out})\,, \tag{13}$$

According to (A.2), we have:

$$\rho_{cost-robust}{}^{hex,mst} = \frac{Num_{mst}^{hex}}{2 \cdot (K-1)} = \frac{1}{2} \cdot n_{opt}(2 \cdot 3^{-\frac{1}{4}} \cdot \lambda_{hex}^{-\frac{1}{2}}, p_{coil}^{out}), \tag{14}$$

Assuming that each wireless node has an independent and identical probability of failure p_{node}^{fail} while the tolerable outage probability for each MI waveguide is p_{coil}^{out}. Then we can approximately evaluate the outage probability of the entire network, i.e. the probability that the data transmission from an arbitrary source to an arbitrary destination is failed due to the disconnected network. For an h-hop transmission, the outage probability $p_{hex}^{out}(h)$ is

$$p_{hex,mst}^{out}(h) = 1 - (1 - p_{node}^{fail})^h \cdot (1 - p_{coil}^{out})^h. \tag{15}$$

According to (14), the outage probability for any transmission is at least $p_{node}^{fail} + p_{coil}^{out} - p_{node}^{fail} \cdot p_{coil}^{out}$ for single hop and can easily approach 1 when the hop number increases. Since the average transmission hop is large in the minimum spanning tree topology, the average outage probability of the network constructed by the MST algorithm is extremely large.

2) Voronoi-Fermat (VF) Algorithm for MI Waveguide Deployment: The Voronoi-Fermat algorithm in the network with hexagonal tessellation topology is much more straightforward than in the random distributed network. The links of the Voronoi diagram-based route are exactly the edges of the hexagonal tessellation while the Fermat point of each equilateral triangle cell is located at the centroid. In the constructed MI-based network, each wireless node has exactly 6 neighbors, which is much more than the MST algorithm (2 neighbors). The cost-robust factor $\rho_{cost-robust}{}_{VF}^{hex}$ can also be derived in the same ways as in the MST algorithm. Therefore,

$$\rho_{cost-robust}{}^{hex,VF} = \frac{Num_{VF}^{hex}}{2 \cdot 3K} = \frac{1}{4} \cdot n_{opt}(4 \cdot 3^{-\frac{3}{4}} \cdot \lambda_{hex}^{-\frac{1}{2}}, p_{coil}^{out}), \tag{16}$$

The outage probability of the network constructed by the VF algorithm can be approximated calculated by summing up the isolated probabilities of the transmitter and the receiver, i.e.

$$p_{hex,VF}^{outage} \simeq 2 \cdot (p_{node}^{fail} + p_{coil}^{out} - p_{node}^{fail} \cdot p_{coil}^{out})^6. \tag{17}$$

It should be noted that this outage probability is applicable for any source-destination pairs disregarding how far they are apart from each other. By comparing the results given in (14)-(17), we can clear see that the Voronoi-Fermat (VF) algorithm achieves much larger neighbor number (node degree), lower cost-robust factor (i.e. higher cost-robust efficiency), and dramatically lower outage probability than the minimum spanning tree (MST) algorithm.

IV. Numerical Evaluation

In this section, we numerically evaluate the required relay coil number and the network robustness of the MST algorithm and the VF algorithm in MI-based networks with both random node distribution and the hexagonal tessellation topology. In the following simulations, 100 wireless nodes are deployed in a square area according to the hexagonal tessellation topology or the homogenous Poisson point process. The size of the square area is determined by the node density. The relay coil number for each MI waveguide is determined by (9)-(11), where the MI waveguide parameters are the same as the parameters used in Section III-A; the displacement intensity of the relay coils is set to be 10%; and the tolerable outage probability for each MI waveguide is set to be 5%.

Fig. 6 shows the deployment results of the MST algorithm and the VF algorithm. The network constructed by the Voronoi

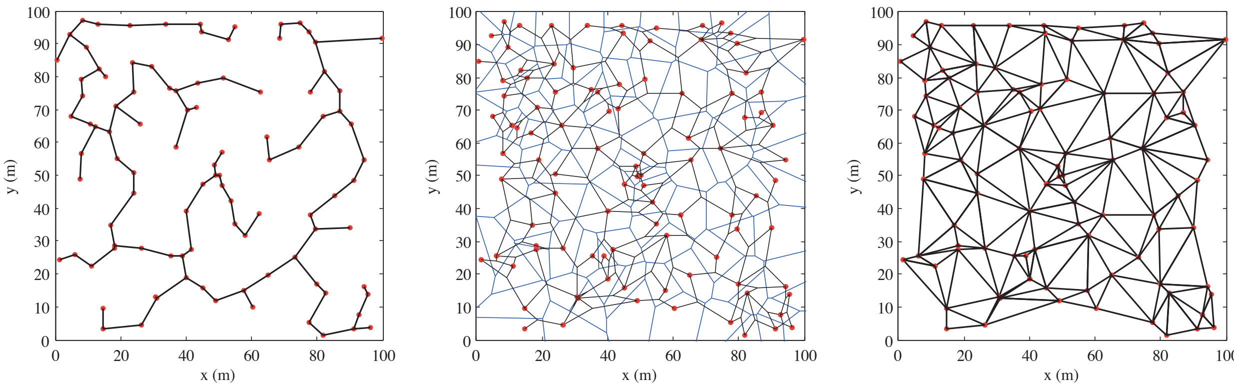

(a) (b) (c)

Fig. 6. The deployment results of (a) the MST algorithm, (b) the VF algorithm, and (c) the VF strategy without the Fermat improvement. (The red dots are the wireless nodes; the black lines represent the MI waveguides; and the blue cells are the Voronoi diagrams. 100 wireless nodes are uniformly distributed with of a spatial intensity $\lambda_{rand} = 0.01\ m^{-2}$.)

diagram-based route without the Fermat improvement is also listed for comparison. Note that the deployment result in the hexagonal tessellation topology is omitted due to its simplicity and the page limit. As shown in the Fig. 6(a), the network constructed by the MST algorithm has the least number of links. Consequently, the relay coil number is small but the network in not robust. The failure of any nodes or the outage of any MI waveguide will result in a disconnected network. In contrast, as shown in Fig. 6(b) and 6(c), the networks constructed by the VF algorithm and Voronoi diagram-based route have the same network topology, which have much more links connecting adjacent wireless nodes. Therefore, the resulted networks are much more robust to node failures but may consume more relay coils.

In Fig. 7(a) and Fig. 7(b), the total relay coil numbers of the deployment algorithms are given as a function of the node density in networks with hexagonal tessellation topology and random node distribution, respectively. Compared with the MST algorithm, the relay coil number required by the VF algorithm is almost the same in the networks with hexagonal tessellation topology and slightly higher in the networks with random node distribution. In both network topologies, the coil number required by the Voronoi diagram-based route is much larger. Next, to see whether the more relay coils bring higher robustness or not, we check the robustness of the networks constructed by VF algorithm and the Voronoi diagram-based route.

In Fig. 8, we exam the network outage probability, i.e., the probability that the data transmission of an arbitrary source-destination pair is failed due to the network connectivity. The network outage probability of the networks constructed by different deployment algorithms are plotted as functions of the failure probability of any single wireless node. It shows that the outage probabilities of the MST algorithm in both hexagonal tessellation topology and the random topology are similar and are close to 1 in such large scale networks (100 nodes). In contrast, the network built by the VF algorithm has extremely low outage probability in large scale networks, especially in the hexagonal tessellation topology network since every node in such networks are guaranteed to have 6 neighbors. It should be noted the outage behavior of the

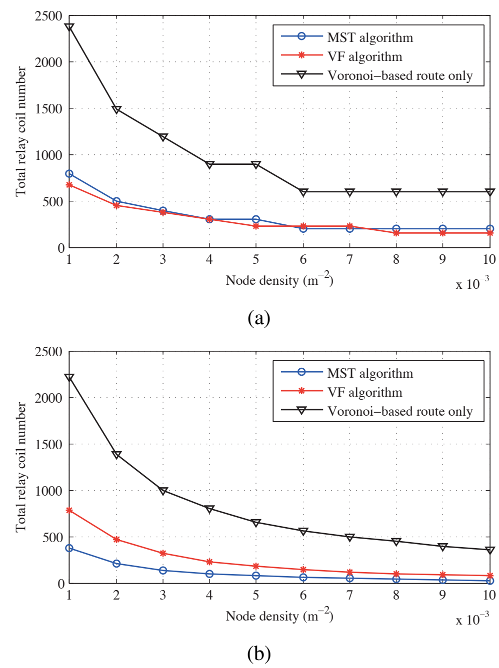

Fig. 7. The number of relay coils to construct a MI-based network with (a) hexagonal tessellation topology and (b) random topology.

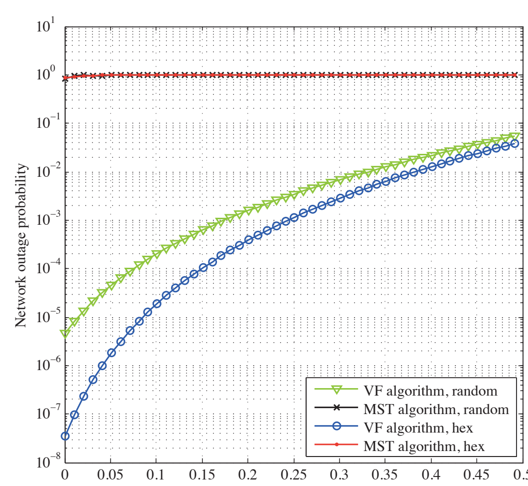

Fig. 8. The network outage probability.

Voronoi diagram-based route is the same as the VF algorithm due to the same link topology.

According to the theoretical and numerical results provided in this section and Section III-B, the MST algorithm can construct a MI-based network with the minimum number of relay coils but the robustness to node failure and coil displacement is extremely poor. Meanwhile, the VF algorithm can greatly enhance the network robustness by just adding a small number of relay coils (even no more coils are needed in the hexagonal tessellation topology).

V. Conclusion

For wireless networks in challenged environments, the MI waveguides solves the propagation problems encountered by the traditional EM wave techniques. This paper investigates the deployment of those MI waveguides to connect the wireless nodes in such networks. In 1D MI-based networks, we analyze the optimal number of relay coils between two adjacent nodes under the impact of coil position deviations. Based on the results in 1D network, we provide two solutions to deploy the MI waveguides in 2D MI-based network. To minimize the relay coil number, the MST algorithm is provided. The MST algorithm uses the minimum spanning tree to connect all the wireless node with the optimal relay coil number. However, the network constructed by the MST algorithm is not robust at all to node failure and coil displacement. To enhance the network robustness while not increasing the relay coil number too much, the VF algorithm is proposed. In VF algorithm, the MI-based network is first established by the Voronoi diagram-based route. Then the Fermat point-based improvement is proposed to further reduce the relay coil number by utilizing the MI waveguides with the shape of the three-pointed star centered at the Fermat point of each triangle cell. The VF algorithm can greatly enhance the network robustness without inducing high deployment cost. Moreover, the constructed network is also efficient in routing and energy consumption due to the planar and spanner properties.

Appendix A
Proof of Proposition 1

Proof: According to the Voronoi diagram-based route, the nodes in the adjacent Voronoi cells are connected to each other. Therefore, the node degree is in fact the side number of the Voronoi cells. The random side number m of the Poisson Voronoi diagram can be approximately modeled by a Gamma distribution [21]. The probability density function (PDF) is given by:

$$f_m(x) \simeq x^{c-1} \cdot b^c \cdot \frac{e^{-bx}}{\Gamma(c)}, \quad x \geq 0 \tag{A.1}$$

where $\Gamma(x)$ is the Gamma function; b and c are constant derived by Monte Carlo estimates in [21]: $b = 3.13$ and $c = 19.784$. Hence, the average node degree is $E(m) = c/b \simeq 6$. ■

Appendix B
Proof of Proposition 2

Proof: According to the definition of the cost-robust factor, we have

$$\rho_{cost-robust} = \frac{\frac{\text{total coil number}}{\text{total node number}}}{\frac{\text{total neighbor number}}{\text{total node number}}} = \frac{\text{total coil number}}{2 \cdot \text{total link number}} = \frac{1}{2} \cdot N_{link}^{coil}. \tag{A.2}$$

According to (A.2), $\rho_{cost-robust}$ is actually determined by the average coil number per link N_{link}^{coil}. In the Voronoi diagram-based route, the resulted network forms a Delaunay triangulation. The minimum spanning tree is a subgraph of the Delaunay triangulation. Due to the homogeneous nodes distribution, the average coil number per link for the two types of network topologies should be in the same order. Besides the above straightforward description, the proposition can also be proved in a more rigorous way: According to Section III-A, the optimal coil number per link is a monotonically increasing function of the link length and the function is approximately linear. Then comparing the average coil number per link is equivalent to compare the average link length of the two types of network topologies. As stated before, the wireless nodes are randomly distributed according to a Poisson process with intensity λ_{rand}. Then the average length of the link in the Delaunay triangulation on those wireless nodes are given by [22]:

$$\overline{L}_{DT} = \frac{32}{9\pi\sqrt{\lambda_{rand}}}, \tag{A.3}$$

The average length of the minimum spanning tree on such nodes can be calculated as [23]:

$$\begin{aligned}\overline{L}_{MST} &= C_2 \cdot (\lambda_{rand} \cdot S_{\mathbb{R}^2})^{\frac{1}{2}} \cdot \int_{\mathbb{R}^2} \left(\frac{1}{S_{\mathbb{R}^2}}\right)^{\frac{1}{2}} dx \cdot \frac{1}{\lambda_{rand} \cdot S_{\mathbb{R}^2}} \\ &= C_2 \cdot \frac{1}{\sqrt{\lambda_{rand}}},\end{aligned} \tag{A.4}$$

where C_2 is a constant; $\mathbb{R}^2$ is the region where the wireless nodes are deployed and $S_{\mathbb{R}^2}$ is its area. Comparing (A.3) with (A.4) completes the proof. ■

Appendix C
Proof of Proposition 4

Proof: In the network constructed according to the Voronoi diagram-based route, we consider an arbitrary transmitter and receiver pair with the Euclidean distance d_E. Assuming that the lengths of the links along the shortest path connecting these two nodes are $\{d_1, d_2, ..., d_J\}$. To prove the power spanner property, we assume that the relay coil density is fixed and the interval between adjacent coils is r_{fix}. Then according to (4), the minimum power consumption (in watt) in the direct transmission for correctly receiving is:

$$P_t^{dir} = 4P_r^{min} \cdot \left(\frac{R}{\omega M}\right)^{2d_E/r_{fix}}, \tag{A.5}$$

where P_r^{min} is the minimum power for correct receiving. For the multihop transmission along the shortest path in the

Voronoi diagram-based route, the minimum power consumption (in watt) is:

$$P_t{}^{path} = \sum_{j=1}^{J} 4P_r^{min} \cdot \left(\frac{R}{\omega M}\right)^{2d_j/r_{fix}}, \tag{A.6}$$

Then the power stretch factor of the constructed network with respect to the complete graph is:

$$\rho_P = \frac{P_t{}^{path}}{P_t{}^{dir}} = \frac{\sum_{j=1}^{J}\left[(\frac{R}{\omega M})^{2/r_{fix}}\right]^{d_j}}{\left[(\frac{R}{\omega M})^{2/r_{fix}}\right]^{d_E}}, \tag{A.7}$$

Since $\frac{R}{\omega M}$ is large enough due to the low coil density, the term $(\frac{R}{\omega M})^{2/r_{fix}}$ is a positive number larger than 1. Then $f(d) = \left[(\frac{R}{\omega M})^{2/r_{fix}}\right]^d$ is an increasing exponential function of d. In addition, according to Proposition 3, $\frac{\sum d_i}{d_E} \leq k$ where $k < \infty$. Since the increasing exponential function is convex, the power stretch factor $\rho_P < k$, too, which completes the proof. ■

Acknowledgment

This work was supported by the US National Science Foundation No. CCF-0728889.

References

[1] I. F. Akyildiz, Z. Sun, and M. C. Vuran, "Signal propagation techniques for wireless underground communication networks," *Physical Commun. J.*, vol. 2, no. 3, pp. 167–183, Sept. 2009.

[2] Z. Sun and I. F. Akyildiz, "Magnetic induction communications for wireless underground sensor networks," *IEEE Trans. Antennas Propag.*, vol. 58, no. 7, pp. 2426–2435, July 2010.

[3] Z. Sun and I. F. Akyildiz, "Underground wireless communication using magnetic induction," in *Proc. 2009 IEEE ICC*.

[4] Z. Sun and I. F. Akyildiz, "Deployment algorithms for wireless underground sensor networks using magnetic induction," in *Proc. 2010 IEEE Globecom*, Best Paper Award.

[5] M. D. Berg, O. Cheong, M. Kreveld, and M. Overmars, *Computational Geometry: Algorithms and Applications*, 3rd edition. Springer, 2000.

[6] Z. Sun, *et.al.*, "BorderSense: border patrol through advanced wireless sensor networks," in *Ad Hoc Netw. J.*, vol. 9, no. 3, pp. 468–477, May 2011.

[7] Z. Sun, *et.al.*, "MISE-PIPE: magnetic induction-based wireless sensor networks for underground pipeline monitoring," *Ad Hoc Netw. J.*, vol. 9, no. 3, pp. 218–227, May 2011.

[8] Z. Sun and I. F. Akyildiz, "On capacity of magnetic induction-based wireless underground sensor networks," in *Proc. 2012 IEEE INFOCOM*.

[9] R. Bansal, "Near-field magnetic communication," *IEEE Antennas Propag. Mag.*, Apr. 2004.

[10] R. R. A Syms, I. R. Young, and L. Solymar, "Low-loss magneto-inductive waveguides," *J. Physics D: Appl. Physics*, vol. 39, pp. 3945–3951, 2006.

[11] V. A. Kalinin, K. H. Ringhofer, and L. Solymar, "Magneto-inductive waves in one, two, and three dimensions," *J. Appl. Physics*, vol. 92, no. 10, pp. 6252–6261, 2002.

[12] M. C. K. Wiltshire, E. Shamonina, I. R. Young, and L. Solymar, "Dispersion characteristics of magneto-inductive waves: comparison between theory and experiment," *Electron. Lett.*, vol. 39, no. 2, pp. 215–217, 2003.

[13] R. Ramanathan and R. Hain, "Topology control of multihop wireless networks using transmit power adjustment," in *Proc. 2000 IEEE INFOCOM*.

[14] M. Burkhart, P. von Rickenbach, R. Wattenhofer, and A. Zollinger, "Does topology control reduce interference?" in *Proc. 2004 ACM MobiHoc*.

[15] J. Pan, T. Hou, L. Cai, Y. Shi, and S. Shen, "Topology control for wireless sensor networks," in *Proc. 2003 ACM MobiCom*.

[16] Y. Wang, "Topology control for wireless sensor networks," in *Wireless Sensor Netw. Appl.: Signals Commun. Technol.*, Y. Li, M. T. Thai, and W. Wu. Springer, 2008, pp. 113–147.

[17] Y. Zou and K. Chakrabarty, "Sensor deployment and target localization based on virtual forces," in *Proc. 2003 IEEE INFOCOM*.

[18] G. Wang, G. Cao, and T. F. La Porta, "Movement-assisted sensor deployment," *IEEE Trans. Mobile Comput.*, vol. 5, no. 6, pp. 640–652, June 2006.

[19] C. P. Dettmann and O. Georgiou, "Product of *n* independent uniform random variables," *Statistics Probability Lett.*, vol. 79, no. 24, pp. 2501–2503, Dec. 2009.

[20] B. Y. Wu and K.-M. Chao, *Spanning Trees and Optimization Problems*. Chapman & Hall/CRC, 2004.

[21] A. L. Hinde and R. E. Miles, "Monte Carlo estimates of the distributions of the random polygons of the Voronoi tessellation with respect to a Poisson process," *J. Statist. Comput. Simul.*, vol. 10, pp. 205–C223, 1980.

[22] R. E. Miles, "On the homogeneous planar Poisson point process," *Mathematical Biosciences*, vol. 6, pp. 85–127, 1972.

[23] J. M. Steele, "Growth rates of Euclidean minimal spanning trees with power weighted edges," *Annals Probability*, vol. 16, no. 4, pp. 177–1787, 1988.

Zhi Sun (M'11) received the B.S. degree in Telecommunication Engineering from Beijing University of Posts and Telecommunications (BUPT), and the M.S. degree in Electronic Engineering from Tsinghua University, Beijing, China, in 2004 and 2007, respectively. He received the Ph.D. degree in Electrical and Computer Engineering from Georgia Institute of Technology, Atlanta, GA. in 2011. Currently, he is Assistant Professor in the Electrical Engineering Department at State University of New York at Buffalo, Buffalo, NY. Prior to that, he was a Postdoctoral Fellow at Georgia Institute of Technology, Atlanta, GA. Dr. Sun has won the Best Paper Award in the 2010 IEEE Global Communications Conference (Globecom). He received the BWN researcher of the year award at Georgia Institute of Technology in 2009. He was also given the outstanding graduate award at Tsinghua University in 2007. His expertise and research interests lie in wireless communications, wireless sensor networks, and cyber physical systems in challenged environments. He is a member of the IEEE.

Ian F. Akyildiz (M'86-SM'89-F'96) received the B.S., M.S., and Ph.D. degrees in Computer Engineering from the University of Erlangen-Nürnberg, Germany, in 1978, 1981 and 1984, respectively. Currently, he is the Ken Byers Chair Professor with the School of Electrical and Computer Engineering, Georgia Institute of Technology, Atlanta, the Director of the Broadband Wireless Networking Laboratory and the Chair of the Telecommunications Group at Georgia Tech. In June 2008, Dr. Akyildiz became an honorary professor with the School of Electrical Engineering at Universitat Politècnica de Catalunya (UPC) in Barcelona, Spain. He is also the Director of the newly founded N3Cat (NaNoNetworking Center in Catalunya). He is also an Honorary Professor with University of Pretoria, South Africa, since March 2009. He is the Editor-in-Chief of *Computer Networks* (Elsevier) Journal, and the founding Editor-in-Chief of the *Ad Hoc Networks* (Elsevier) Journal, the *Physical Communication* (Elsevier) Journal and the *Nano Communication Networks* (Elsevier) Journal. Dr. Akyildiz serves on the advisory boards of several research centers, journals, conferences and publication companies. He is an IEEE Fellow (1996) and an ACM Fellow (1997). He received numerous awards from IEEE and ACM. His research interests are in wireless sensor networks, cognitive radio networks, and nanonetworks.